High-Pressure Falling Sphere Viscosimetry of Basaltic and Dacitic Rocks in Conjunction with Synchrotron Radiation

Hans J. Mueller[1], N. Stroncik[1], R. Naumann[1], C. Lathe[1], M. Spiwek[2] ,

M. Wehber[1], F.R. Schilling[3], J. Lauterjung[1]

[1]GFZ German Research Centre for Geosciences, Telegraphenberg, D-14473 Potsdam, Germany

[2]Deutsches Elektronen-Synchrotron DESY, Notkestrasse 85, D-22607 Hamburg, Germany

[3]University of Karlsruhe, Geologisches Institut, D-76128 Karlsruhe, Germany

hjmuel@gfz-potsdam.de

Abstract. In situ falling-sphere technique viscosity measurements in a DIA-type multi-anvil apparatus - MAX80 at beamline F2.1 at DESY / HASYLAB, Hamburg, Germany - have been performed. The viscosity was measured following Stokes law by evaluation of X-radiography sequences taken by a CCD-camera. Powdered basalt, dacite, and diabase samples were measured at pressures of 0.5 and 1 GPa and temperatures of 1890 K. After pressurization the temperature produced by an internal graphite heater was increased up to sample melting observed by X-ray diffraction and X-radiography. The results cover a data range from 3.5 Pa s (basalt at 1 GPa) and 195.5 Pa s (diabase at 0,5 GPa) and are in good agreement with published data.

1. Introduction

The viscosity of silicate melts is of vital importance for the transport of mass and energy inside the Earth. Using short- and long-period precursors of PKP phases ultra-low velocity zones (ULVZ) even at the core-mantle boundary beneath the Western Pacific (Wen and Helmberger, 1998) and central Africa (Ni and Helmberger, 2001) were observed. The elastic properties of these zones correspond to partial molten state. In spite of resolving problems recent geophysical data result in a rising indication for a relation of the base of superplumes to these thermo-chemical piles (Kellogg et al., 1999; Romanowicz and Gung, 2002; Lassak et al., 2007). To understand the differentiation processes in the Earth's interior quantitatively data on the physical properties of melts, viscosity in particular, are crucial.

Multi-anvil apparaus (MA), also known as large volume presses (LVP), have been proved to be highly succesful tools for measuring the physical properties of Earth's materials under experimentally simulated mantle conditions. First falling sphere viscosimetry was successfully used in quench experiments (e.g. Kushiro, 1976, 1978; Kushiro et al., 1976) using piston cylinder devices, later also with multi-anvil apparatus (Knoche & Luth, 1998; Mori et al., 2000). But this technique require a

sequence of quench experiments to measure the viscosity of one sample and the time resolution is limited because of the heat capacity of the set-up with the adjacent anvils. The installation of large volume presses at synchrotron X-ray facilities represented a huge progress for in-situ viscosity measurements, because the falling sphere could be observed and monitored in real time now. This eliminated the problems of accurately determining time-distance-relationships of the quench experiments. Additionally by placing a pressure standard close to the sample inside the set-up the pressure could be determined much more precisely by X-ray diffraction (Kanzaki et al., 1987; Dobson et al., 1996, 2000; Rutter et al., 2002; Secco et al., 2002; Suzuki et al., 2002; Tinker et al, 2004; Hui et al., 2009). The common way of saving the falling sphere movie is an analog technique, i.e. using a videotape. That sets the frame rate to 50 (PAL, SECAM) or 60 (NTSC) half-frames per second in dependence on the television standard of the equipment. Meantime the improved sensitivity of CCD-cameras in coincidence with the increased energy level of recent synchrotron insertion devices allows pure digital techniques, i.e. the frame rate can be freely decided in dependence on the requirements of the measurement.

We used powdered glass samples of basalt, dacite, and diabase for our experiments. The basalt and the dacite samples were dredged along the neo-volcanic zone of the Pacific-Antarctic-Rise during the SONNE 157 cruise. They were chosen for the conducted experiments because they represent compositional extremes in magmatic evolution and thus also a large diversity considering the rheological properties of magmas such as viscosity and yield strength. Both samples plot along the same path of fractional crystallisation and therefore characterize different evolutionary stages of the magma they developed from. Sample 53DS5 consists of a relatively primitive basalt having a Mg/Mg+Fe of 63 and a SiO_2 content of 49.37 wt.%, whereas sample 65DS3 is highly evolved, consisting of a dacite with an Mg/Mg+Fe of 14 and a SiO_2 content of 67.80 wt.%. Both samples are also characterized by a highly different volatile content. Sample 53DS5 contains 0.2 wt.% H_2O and 80 ppm Cl, whereas sample 65DS3 contains about 3.2 wt.% H_2O and 8400 ppm Cl. The diabase (standard sample BM) was sampled at the quarry of Mellenbach, close to Grossbreitenbach (Thuringia, Germany). The main constituent minerals are albite, chlorite, and hornblende with some calcite as fissure mineral. The chemical composition is 49.51 wt.% SiO_2, 16.25 wt.% Al_2O_3, 1.6 wt.% Fe_2O_3, 7.28 wt.% FeO, 0.14 wt.% MnO, 7.47 wt.% MgO, 6.47 wt.% CaO, 4.65 wt.% Na_2O, 0.2 wt.% K_2O, and 1.14 wt.% Ti_2O.

2. Experimental methods

The experiments were performed in the single-stage multi-anvil DIA-device MAX80 installed at beamline F2.1 at DESY / HASYLAB, Hamburg; Germany (Mueller et al., 2005a, b, 2006, 2007). The apparatus is made up of a 2500 N hydraulic ram with two load frames driving four reaction bolsters for the lateral anvils (Fig. 1). For these experiments we used a tungsten carbide anvil set with 6 mm truncation. The maximum pressure of about 7 GPa corresponds to the measurement problem. The maximum temperature is about 2000 K.

The pressure measurement was carried out by energy-dispersive X-ray diffraction (XRD) using MgO corresponding to the Equation of state (EOS) by Speziale et al., 2001. A Ge-solid-state detector recorded the diffracted beam at a fixed 2θ angle of 8°. For switching between XRD and X-radiography MAX80 is equipped with a four-blade high-precision slit system of Advanced Design Consulting USA, Inc.ADC). The maximum slit opening is 1 inch. Because the 4 blades can be moved independently from each other, the slits system is not only able to control the beam size, but it can also define the X-ray beam position. For X-radiography of the falling sphere the vertical opening of the slits should cover more than the entire drop height inside the sample capsule. We put it to about 2.5 mm. Using tungsten carbide anvils absorbing the synchrotron radiation the maximum horizontal opening is adapted to the maximum available gap between the lateral anvils, about 1,5 to 0.5 mm in dependence on pressure.

After penetrating the high pressure cell assembly, the X-ray shadow graph is partially converted by fluorescence of a 0.1 mm-thick Ce: YAG-crystal (by courtesy of Institut für Kristallzüchtung – IKZ) to an optical image of ~540 nm wavelength (green). An aluminum-coated mirror decouples the optical from the non-converted X-ray image, which is absorbed in the beam-stop (Fig. 2). We used a Leica Z 16 APO A 16 : 1 motorized zoom macroscope for the magnification of the optical images. Finally the images are captured by a Leica DFC 350 FX high-sensitivity 12-bit monochrome 1.4 Megapixels CCD-camera. Active cooling of sensor elements using a Peltier element creates noise-free images even at the lowest light intensities. The maximum frame rate is at 60 frames per second (fps). The captured images are transferred to a PC by standard Fire Wire (Fig. 3).

Fig. 4 shows the cross section of the set-up. An 8 mm boron epoxy cube contains the stepped graphite heater with two copper rings for current supply. The rock samples were grounded to a < 30 µm powder in a mortar and pestle. The sample powder dried at 120°C was firmly packed into the graphite capsule. Close to the top of the filled capsule a platinum sphere was placed in the centre and covered with a thin layer of sample powder before the capsule was closed by the graphite top cover. The Pt spheres were formed by melting from a 0.1 mm Pt wire using a hydrogen microburner. The sphere diameter was determined with a measuring microscope. We found diameters between 0.26 and 0.333 mm. The capsule is separated from the surrounding heater by a boron nitride sleeve. Adjacent to the sample capsule the MgO standard for pressure measurement is located. The set-up is completed by a blow-out preventer made from fired pyrophyllite at one side and by an Al_2O_3-4-hole capillary tube for the thermocouple wires at the opposite side. We used a $W_{97\%}\,Re_{3\%}$ - $W_{75\%}\,Re_{25\%}$ thermocouple and no correction was applied for the effect of pressure on the emf.

The viscosity was measured at pressures of 0.5 and 1 GPa. Each experiment started with compression at roam temperature. Then the temperature was ramped slowly by about 100 K per minute up to the melting point of the sample. Then the temperature was rised much faster by ~ 50 K per second for further 100 K. The falling spheres were monitored by the digital camera with a frame rate of 25 fps. The X-radiography images were analyzed to determine a distance versus time plot of the sphere.

We used a modified Stokes' Law to calculate the viscosity, η.

$$\eta = \frac{2gr^2\Delta\rho}{9\nu}\left[1 - 2.104\left(\frac{r}{r_c}\right) + 2.09\left(\frac{r}{r_c}\right)^3 - 0.95\left(\frac{r}{r_c}\right)^5\right]$$

where g is the gravitational constant, r is the radius of the falling sphere, Δρ is the density contrast between the sphere and the melt, ν is the settling velocity, and r_c is the internal radius of the sample capsule. The term in brackets is the Faxen correction for wall effects on the settling velocity of the sphere (Faxen, 1925; Shaw, 1963).

3. Results and Discussion

The X-radiography movies were analyzed by image processing frame per frame. Fig. 5 shows such a sequence as an example. Between all the displayed images is a time interval of 2 seconds each. Because of the much higher density of the platinum sphere in comparison to the surrounding silicate melt the sphere appears as black. Measuring the position of the sphere at all images of the sequence taken with a constant time interval allows to deduce a distance versus time plot of the falling sphere. Fig. 6 shows such a plot with the reduced time interval of 1 second for demonstration. The sigmoidal shape of the distance data is indicative of the acceleration, terminal velocity, and deceleration phases of the sphere motion. The terminal velocity of the sphere, used to calculate the viscosity of the

samples, was determined as the maximum slope at the centre of the linear part. For the example of Fig. 6 this is at about 8.5 seconds.
Fig. 7 shows our results for basalt, diabase, and dacite at 0.5 GPa and 1 GPa. For the first falling sphere experiment, at the same time the first experiment of this type at DESY / HASYLAB, we used optical lute because it melts at much lower temperatures (150°C to 350°C) than silicate samples. This result measured at 0.5 GPa is also displayed. In addition to our results we display published data. Our results are in very good agreement with the data of Suzuki et al., 2002, Tinker et al., 2004, Mori et al., 2000, and Brearley et al., 1986. Taking into account the much lower temperatures of the experiments of Kushiro, 1978 and Brearley & Montana, 1989 the accordance with these data is also very good. The relatively low viscosity of our dacite sample might probably be the result of the high water and chlorine contents (3.2 wt.% H_2O and 8400 ppm Cl).

4. Conclusions

The in-situ falling sphere technique was used to determine the viscosity of basaltic and dacitic melts at high pressure conditions. The settling velocity of a platinum sphere was measured by analyzing the sequences of X-ray shadowgraphs taken under in-situ conditions. Our viscosity data are in very good agreement with published data in terms of absolute value and negative pressure dependence. The experiments will be continued at higher pressures and including further samples. For pressures higher than 6 GPa MAX200x – a double-stage LVP with a 1750 tons hydraulic press installed at beamline W2 at DESY / HASYLAB – will be used. The X-radiography equipment corresponds to that at MAX80. The large-area high-energy monochromatic X-ray beam there results in a higher resolution of the images. Because higher pressures causes narrower gaps between the anvils the observation of the falling sphere becomes critical. Using x-ray transparent anvil top pieces will make the whole sample visible for X-radiography.

Acknowledgments: The authors would like to acknowledge the kind introduction to the technique and very fruitful discussions with Ch. Lesher, as well as the support by Y. Wang, and D. Dobson. The authors are particularly indebted to B. Meier, G. Tiede, and H. Zink for technical support, as well as M. Kreplin, R. Sünkel, and W. Steiner for their firm involvement in special preparation.

References

[1] Wen L, Helmberger DV 1998 Ultra-low velocity zones near the core-mantle boundary from broadband PKP precursors *Science* vol. 279, no. 5357 pp 1701-1703
[2] Ni S, Helmberger DV 2001 Probing an ultra-low velocity zone at the core mantle boundary with P and S waves *Geophys. Res. Lett,* 28 (12) pp 2345–2348
[3] Kellogg LH, Hager BH and van der Hilst RD 1999 Compositional Stratification in the Deep Mantle *Science* vol. 283, no. 5409 pp 1881-1884
[4] Romanowicz B and Gung YC 2002 Superplumes from the core-mantle boundary to the base of the lithosphere *Science* 296 pp 513-516
[5] Lassak TM, McNamara AK and Zhong S 2007 Influence of thermochemical piles on stress development at Earth's core-mantle boundary *Earth Planet Sci. Lett.* 261 pp 443-455
[6] Kushiro I 1976 Changes in viscosity and structure of melt of $NaAlSi_2O_6$ composition at high pressures *J. Geophys. Res.* 81 pp6347-6350
[7] Kushiro I 1978 Viscosity and structural changes of albite ($NaAlSi_3O_8$) melt at high pressures *Earth Planet. Sci. Lett.* 41 pp 87-90
[8] Kushiro I, Yoder HS, Mysen BO 1976 Viscosities of basalt and andesite melts at high pressures *J. Geophys. Res.* 81 pp 6351-6356
[9] Knoche R and Luth RW 1996 Density measurements on melts at high pressure using sink/float

method: Limitations and possibilities *Chemical Geology* 128 pp 229-243
[10] Mori S, Ohtani E and Suzuki A 2000 Viscosity of the albite melt to 7 GPa at 2000 K *Earth Planet. Science Lett.* 175 pp87-92
[11] Kanzaki M, Kurita K, Fuji T, Kato T, Shimomura O and Akimoto S 1987 A new technique to measure the viscosity and density of silicate melts at high pressure *High Pressure Research in Mineral Physics* Eds MH Manghnani and Y Syono (American Geophysical Union Washington) pp 195-200
[12] Dobson DP, Jones AP, Rabe R, Sekine T, Kurita K, Taniguchi T, Kondo T, Kato T, Shimomura O and Urakawa S 1996 In-situ measurement of viscosity and density of carbonate melts at high pressure *Eárth Planet. Sci. Lett.* 143 pp 207-215
[13] Dobson DP, Crichton WA, Vočadlo L, Jones AP, Wang Y, Uchida T, Rivers M, Sutton S and Brodholt JP 2000 In-situ measurement of viscosity of liquids in the Fe-FeS system at high pressures and temperatures *Am. Mineral.* 85 pp1838-1842
[14] Rutter MD, Secco RA, Liu H, Uchida T, Rivers ML, Sutton SR and Wang Y 2002 Viscosity of liquid Fe at high pressure *Phys. Rev. (B)* 66 pp 060102-2-060102-4
[15] Secco RA, Rutter MD, Balog SP, Liu H, Rubie DC, Uchida T, Frost D, Wang Y, Rivers ML and Sutton SR 2002 Viscosity and density of Fe-S liquids at high pressures *J. Phys..: Condensed Matter* 14 pp 11325-11330
[16] Suzuki A, Ohtani E, Funakoshi K, Terasaki H and Kubo T 2002 Viscosity of albite melt at high pressure and temperature *Phys. Chem. Minerals* 29 pp159-165
[17] Tinker D, Lesher ChE, Baxter GM, Uchida T and Wang Y 2004 High-pressure viscometry of polymerized silicate melts and limitations of the Eyring equation *Am Mineral.* 89 pp 1701-1709
[18] Hui H, Zhang Y, Zhengjiu X, Del Gaudio P and Behrens H 2009 Pressure dependence of viscosity of rhyolitic melts Geochem Cosmochem Acta 73 pp 3680-3693
[19] Mueller HJ, C. Lathe C and Schilling FR 2005a Simultaneous determination of elastic and structural properties under simulated mantle conditions using multi-anvil device MAX80 *Advances in High Pressure Technology for Geophysical Application* Eds J Chen, Y Wang, T Duffy, Shen T and L Dobrzhinetskaya (chapter 4, Elsevier B.V., London/Amsterdam/New York) pp 67-94
[20] Mueller HJ, C. Lathe C, Schilling FR and Lauterjung J 2005b Calibration based on a primary pressure scale in a multi-anvil device *Advances in High Pressure Technology for Geophysical Application* Eds J Chen, Y Wang, T Duffy, Shen T and L Dobrzhinetskaya (chapter 21, Elsevier B.V., London/Amsterdam/New York) pp 427-449
[21] Mueller HJ, Schilling FR, Lathe C and Lauterjung L 2006 Recent development of experimental techniques for high-pressure mineral physics under simulated mantle conditions *High Pressure Research* 26 pp 529-537
[22] Mueller HJ, Schilling FR and Lathe C 2007 Multianvil techniques in conjunction with synchrotron radiation at Deutsches ElektronenSYnchrotron (DESY) – Hamburger Synchrotron LABor (HASYLAB) *Geol. Soc. Am. Special Paper* 421 pp 207-226
[23] Speziale S, Zha Ch, Duffy TS, Hemley RJ and Mao H 2001 Quasi-hydrostatic compression of magnesium oxide to 52 GPa: Implications for the pressure-volume-temperature equation of state J. Geophys, Res. 106 pp 515-528
[24] Faxen H 1925 Gegenseitige Einwirkung zweier Kugeln , die in einer zähen Flüssigkeit fallen *Ark. Mat. Astron. Fys*. 19 pp 1-8
[25] Shaw HR 1963 Obsidian-H 2 O viscosities at 1000 and 2000 bars in the temperature range 700° to 900° C *J. Geophys. Res.* 68 pp 6337-6343
[26] Brearley M, Dickinson JE and Scarfe CM 1986 Pressure dependence of melt viscosities on the join diopside-albite *Geochim. Cosmochim. Acta* 50 pp 2563-2570
[27] Brearley M and Montana A 1989 The effect of CO 2 on the viscosity of silicate liquids at high pressure *Geochim Cosmochim Acta* 53 pp 2609-2616

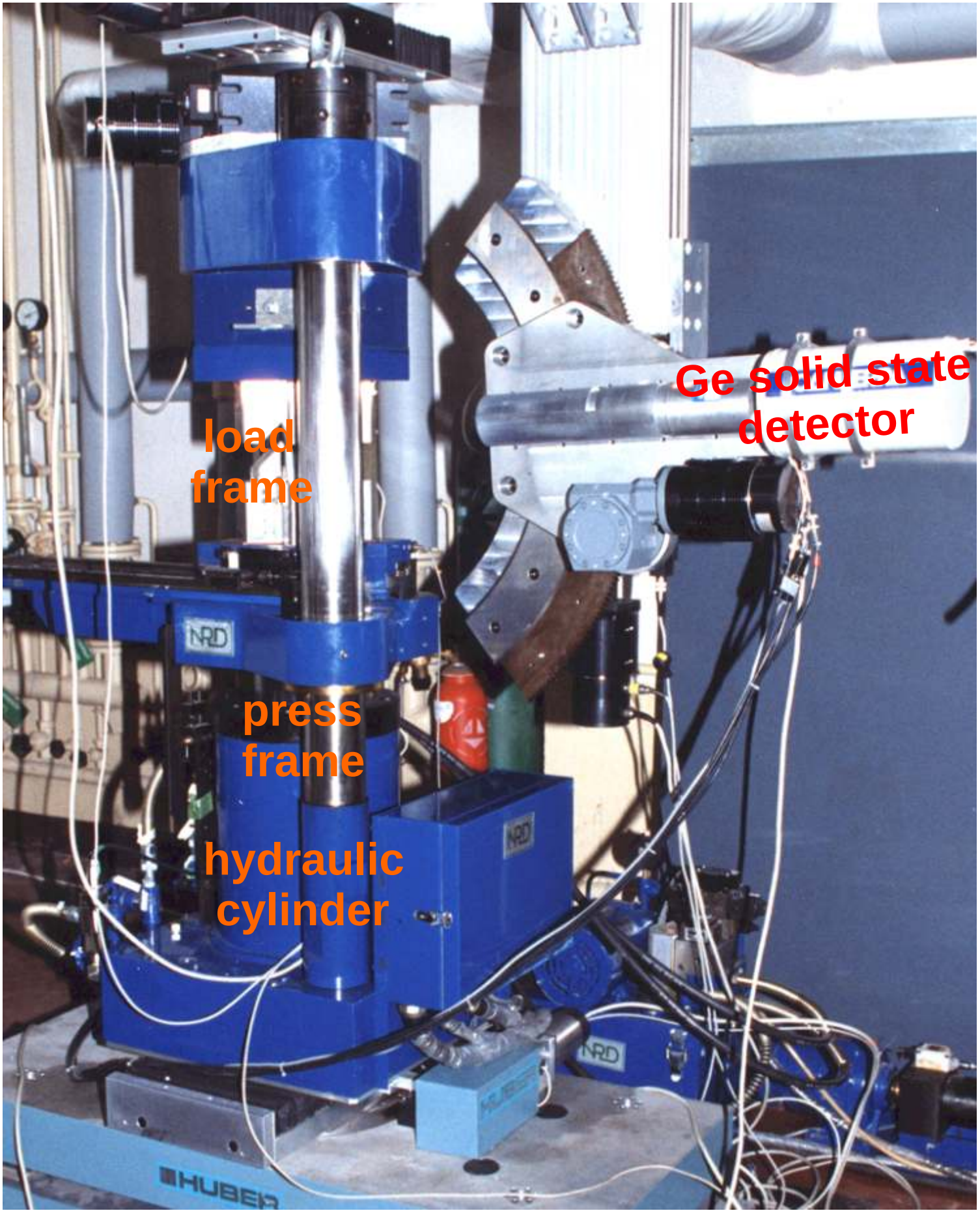

Figure 1. MAX80 at DESY / HASYLAB, Hamburg, Germany beamline F2.1
single-stage multi-anvil apparatus
250 tons hydraulic ram

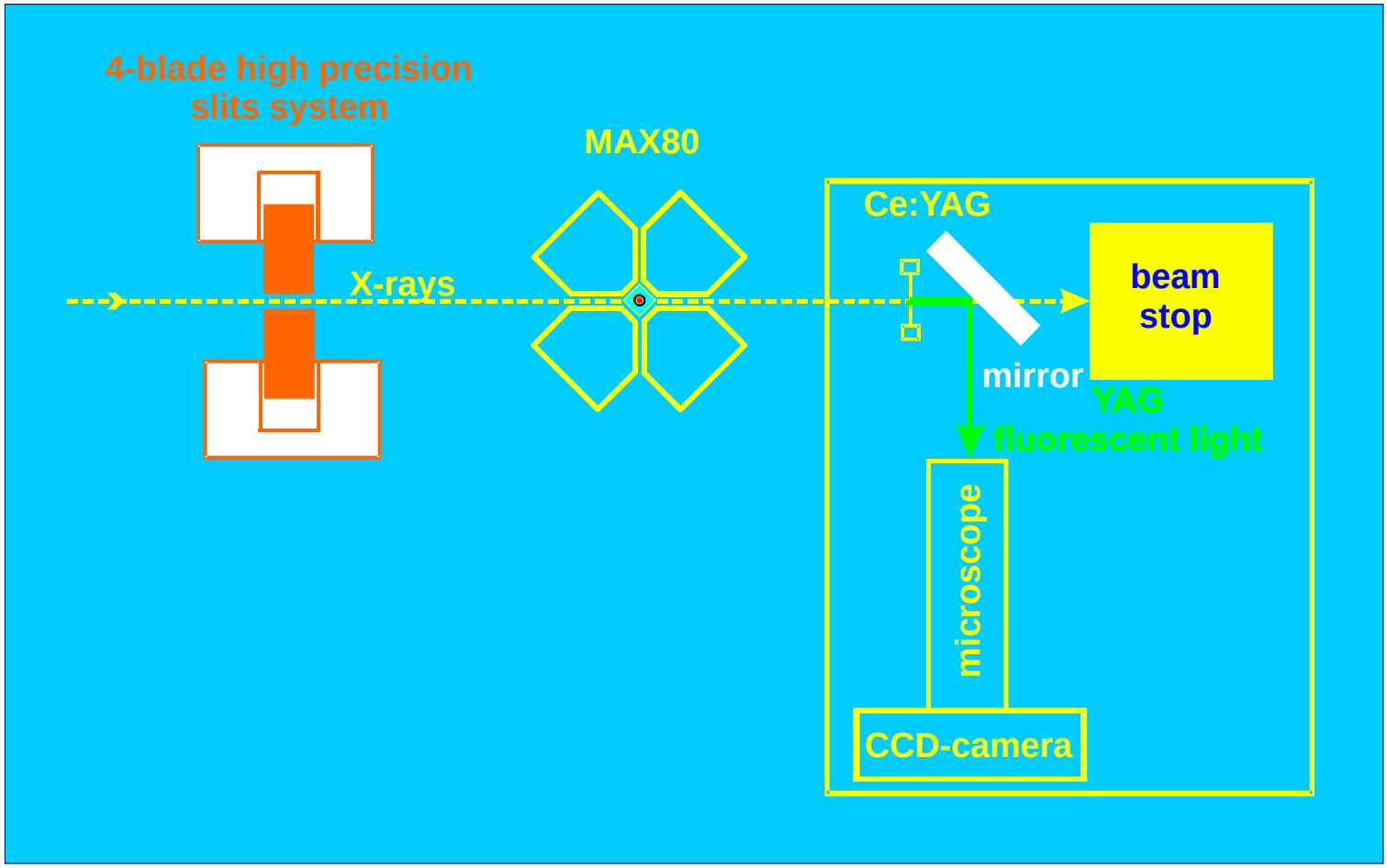

Figure 2. X-radiography set-up for multi-anvil devices - the X-ray image is converted to an optical one by a Ce: YAG-crystal and captured by a macroscope and a CCD-camera.

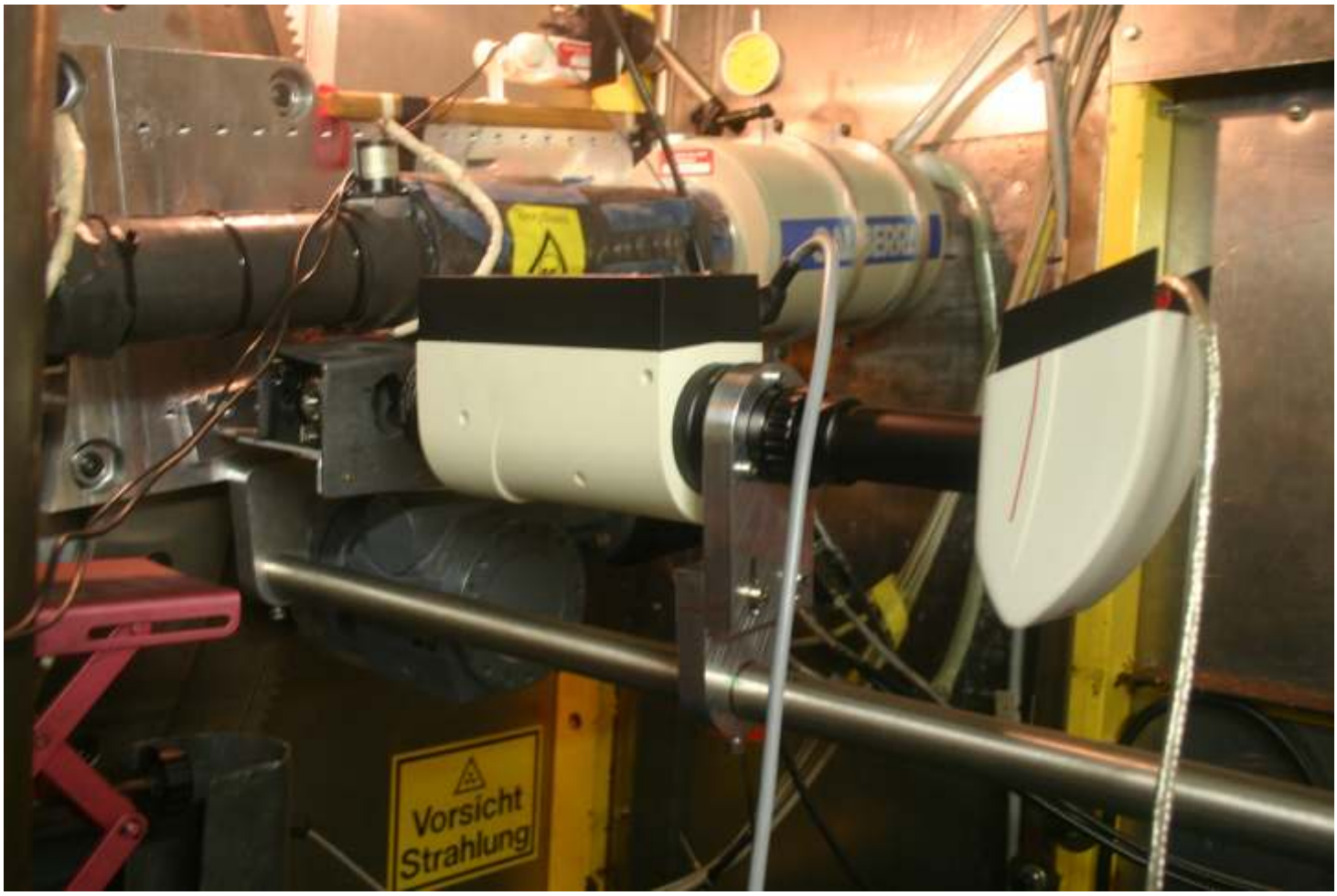

Figure 3. X-radiography set-up at MAX80
The equipment is mounted below the Ge-solid-state detector in the background. The Ce: YAG-crystal is placed in the direct beam.

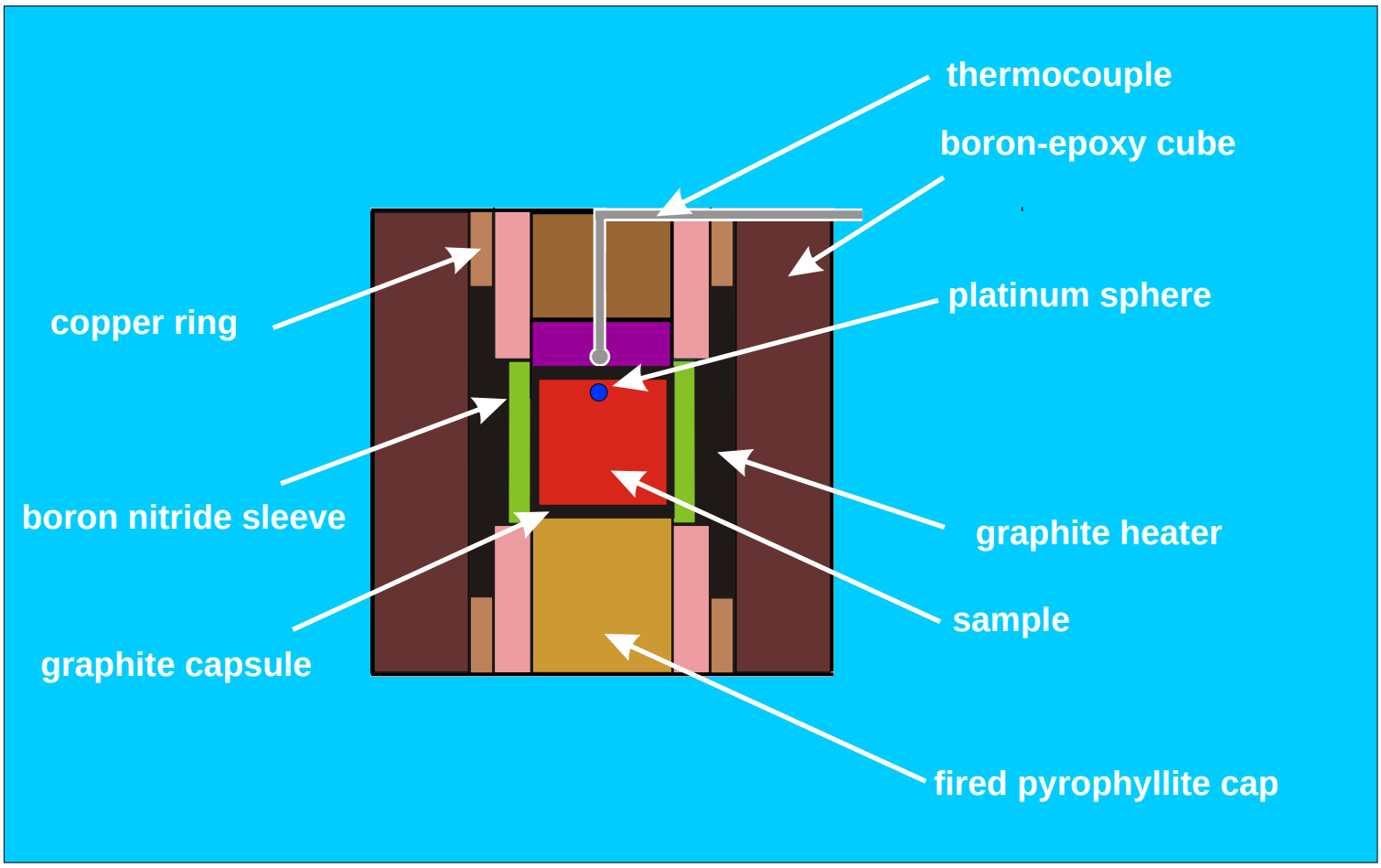

Figure 4. Scheme of falling-sphere viscosimetry set-up at MAX80

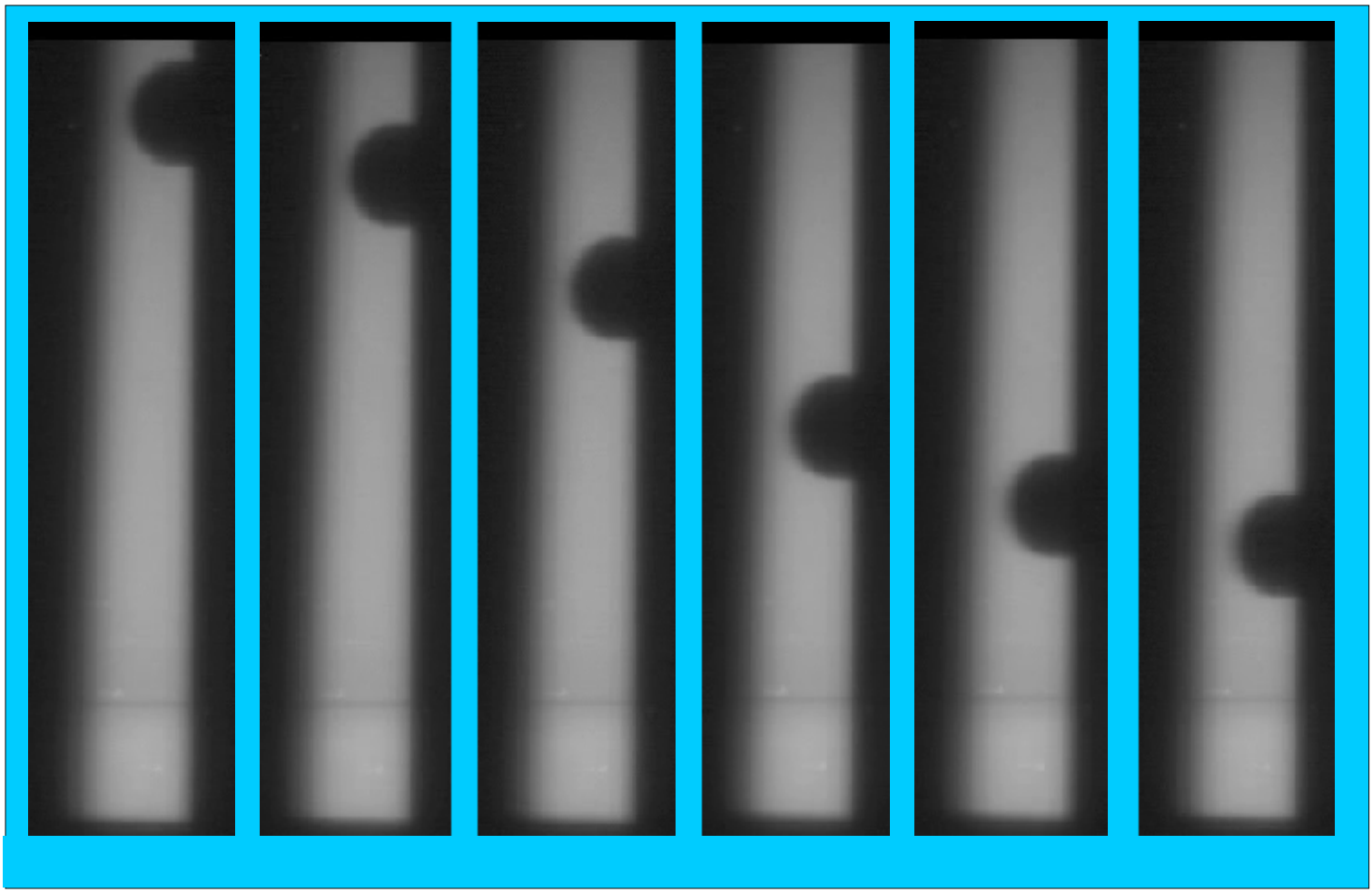

Figure 5. Sequence of falling sphere images with a time interval of 2 seconds

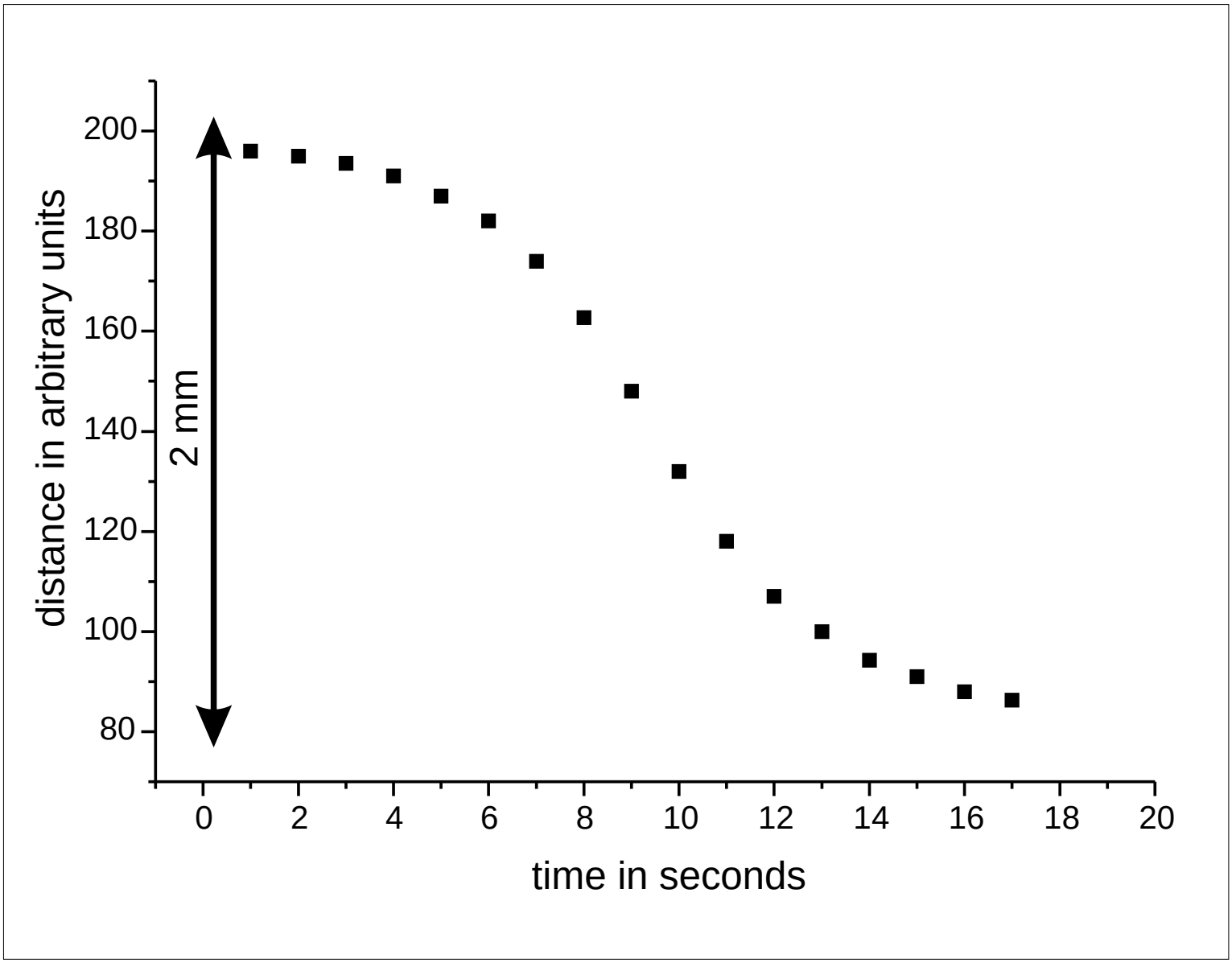

Figure 6. X-radiography falling sphere distance versus time plot

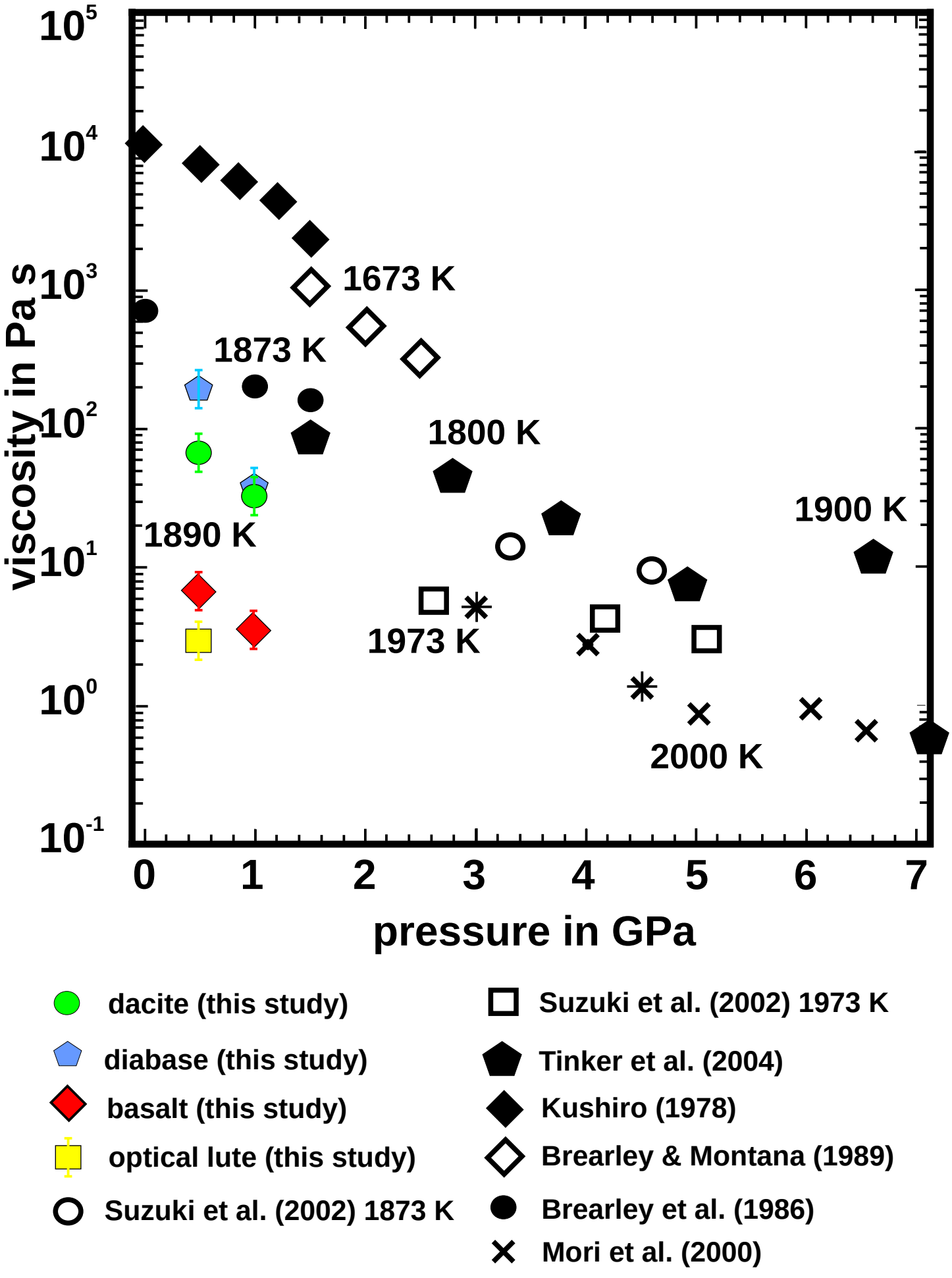

Figure 7. Viscosity of basalt, diabase, and dacite at high pressure and temperature (this work) in comparison to published data